

Characterization of the Short Strong Hydrogen Bond in Benzoylacetone by ab Initio Calculations and Accurate Diffraction Experiments. Implications for the Electronic Nature of Low-Barrier Hydrogen Bonds in Enzymatic Reactions

Birgit Schiøtt,[†] Bo Brummerstedt Iversen,^{*,†,‡} Georg Kent Hellerup Madsen,[§] and Thomas C. Bruice^{*,†}

Contribution from the Departments of Chemistry, University of California at Santa Barbara, Santa Barbara, California 93106, and the University of Aarhus, DK-8000 Århus C, Denmark

Received July 2, 1998

Abstract: The intramolecular hydrogen bond in benzoylacetone has been studied with high-level ab initio Hartree–Fock and density functional theory methods. The results are compared to the experimental structure as obtained from low-temperature neutron and X-ray diffraction experiments. The calculations reveal that electron correlation effects are essential for modeling the experimental low-temperature neutron diffraction structure of benzoylacetone. At the B3LYP/6-311G(d,p) level of theory the intramolecular oxygen–oxygen distance is found to be 2.51 Å and the hydrogen bond energy can be estimated to be 16 kcal/mol. The transition state for intramolecular hydrogen transfer was located with the barrier estimated to be about 2 kcal/mol, consistent with a low-barrier hydrogen bond. Upon addition of the zero-point vibration energies to the total potential energy, the internal barrier vanished, overall suggesting that the intramolecular hydrogen bond in benzoylacetone is a very strong hydrogen bond. Analysis of the electron density with the “atoms in molecules” theory revealed that both oxygen–hydrogen bonds have some covalent character. Theoretical atomic charges and the dipole moment were computed by fitting point charges to the electrostatic potential of the molecule. Excellent quantitative agreement is found for most properties of the charge density whether determined computationally or by X-ray diffraction. Both methods reveal that the oxygen and hydrogen atoms have substantial atomic charges, and consequently the resonance assisted hydrogen bond in benzoylacetone is best described as a 3-center, 4-electron σ -bond with considerable electrostatic as well as covalent bonding contributions. The present study implies that if low-barrier hydrogen bonds (LBHB) are formed in enzymatic reactions, they possess covalency between the hydrogen atom and both heteroatoms in question. Furthermore, it is expected that large atomic charges will be found in the LBHB, which give rise to an additional electrostatic stabilization of the system.

Introduction

The formation of inter- and intramolecular hydrogen bonds has for a long time been recognized as very important in all fields of molecular recognition.¹ The importance of such bonds spans all fields of chemistry from biochemistry² to the design of nanostructured materials (crystal engineering)³ and the self-assembly of large pore zeolites.⁴ Recently, much research has focused on obtaining a better understanding of the nature of the hydrogen bond.⁵ Special attention has been given to short

strong hydrogen bonds as low-barrier hydrogen bonds (LBHB) and they have been incorporated into various enzymatic reaction mechanisms.⁶ Originally, the involvement of LBHBs in enzymatic reactions was put forward by Cleland based on the observation of unusually low hydrogen fractionation factors.^{6a} Immediately thereafter, several enzymes were suggested to take advantage of the formation of LBHBs to stabilize intermediates or transition states in the course of the enzymatic transformation.^{6,7} The proposal initiated a lively debate^{6d–g,7} on the

* To whom correspondence should be addressed. E-mail: bo@kemi.aau.dk or tcbuice@bioorganic.ucsb.edu. Fax: +45 8619 6199 or +1 (805) 893-4120.

[†] University of California.

[‡] Present address: Department of Chemistry, University of Aarhus, DK-8000 Århus C, Denmark.

[§] University of Aarhus.

(1) See the entire 1997 issue 5: *Chem. Rev.* **1997**, 97.

(2) Jeffrey, G. A., Saenger, W. *Hydrogen Bonding in Biological Structures*; Springer: Berlin, 1991.

(3) (a) Aakeroy, C. B. *Acta Crystallogr.* **1997**, B53, 569–586. (b) Desiraju, G. R. *Chem. Commun.* **1997**, 1475–1482.

(4) (a) Feng, P. Y.; Bu, X. H.; Stucky, G. D. *Nature* **1997**, 388, 735–741. (b) Bu, X. H.; Feng, P. Y.; Stucky, G. D. *Science* **1997**, 278, 2080–2085.

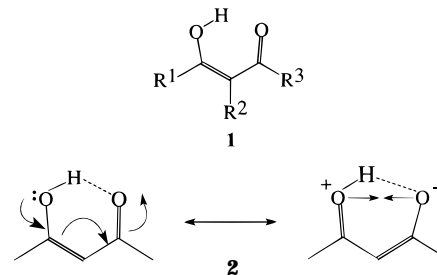
(5) (a) Jeffrey, G. A. *An Introduction to Hydrogen Bonding*; Oxford University Press: New York, 1997. (b) Hibbert, F.; Emsley, J. *Adv. Phys. Org. Chem.* **1990**, 26, 255–379. (c) *Modelling of the Hydrogen Bond*; Smith, D. A., Ed.; ACS Symp. Ser. No 569; American Chemical Society: Washington, DC.

(6) (a) Cleland, W. W. *Biochemistry* **1992**, 31, 317–319. (b) Gerlt, G. A.; Gassman, P. G. *J. Am. Chem. Soc.* **1993**, 115, 11552–11568. (c) Cleland, W. W.; Kreevoy, M. M. *Science* **1994**, 264, 1887–1890. (d) Frey, P. A.; Whitt, S. A.; Tobin, J. B. *Science* **1994**, 264, 1927–1930. (e) Tobin, J. B.; Whitt, S. A.; Cassidy, C. S.; Frey, P. A. *Biochemistry* **1995**, 34, 6919–6924. (f) Cassidy, C. S.; Lin, J.; Frey, P. A. *Biochemistry* **1997**, 36, 4576–4584. (g) Warshel, A.; Papazyan, A.; Kollman, P. A. *Science* **1995**, 269, 104–106. (i) Guthrie, J. P. *Chem. Biol.* **1996**, 3, 163–170. (j) Gerlt, G. A.; Kreevoy, M. M.; Cleland, W. W.; Frey, P. A. *Chem. Biol.* **1997**, 4, 259–267.

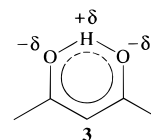
involvement of LBHB in enzymatic catalysis. Most of the dispute concerned the energy gained by formation of a short strong hydrogen bond in the active site of enzymes. In the gas phase, energies of more than 30 kcal/mol have been measured. It was proposed^{6c} that in the enzymatic reaction, the bond energy could be as high as 10–20 kcal/mol, depending strongly on the nature (hydrophobicity, electrostatics, etc.) of the active site.^{6g,i} Warshel *et al.* suggested that electrostatic interactions alone can account for the stabilization energy in enzymatic reactions and, therefore, regarded LBHBs as being of no importance in enzymes.^{6g} Kreevoy, Cleland,^{6h} and others,^{6j} on the other hand, argued that electrostatics alone cannot explain the special physicochemical properties, such as ¹H chemical shift and ν_{OH} , found in some enzymes which all indicate that some degree of charge-redistribution is present in the hydrogen-bonded fragments.

Gilli and co-workers⁸ have examined several small molecular systems with either O \cdots H–O or O \cdots H–N inter- or intramolecular hydrogen bonding. They have categorized the hydrogen bonding according to the total charge of the system as being either negative (–) or positive (+) charge assisted hydrogen bonds (CAHB) or resonance assisted hydrogen bonds (RAHB). In the latter, the hydrogen bond donor and acceptor atoms are connected through π -conjugated double bonds, as in the keto–enol isomers of β -diketones, **1**.^{8a} General trends were found in characterizing short strong hydrogen bonds, as correlations between the strength of the O \cdots H–O bond and the O \cdots O separation^{8b,e} were established. The O \cdots H–O bond strength was estimated either from the high ¹H NMR chemical shifts ($\delta_{\text{H}} = 15\text{--}19$ ppm) or by $\nu(\text{O–H})$.^{8b,e} Traditionally, O \cdots H–O and O \cdots H–N hydrogen bonds are believed to be electrostatic in nature;⁵ however, in the RAHB systems, no formal charges are found at the hydrogen bonded heteroatoms. Gilli *et al.*⁸ suggested that the additional hydrogen bonding energy in the strong RAHB systems can be thought of as originating from partial charges of opposite signs present in the resonance isomer, **2**. They proposed an imaginary two-step synergistic mechanism to explain the formation of an RAHB. In the first step of the mechanism, the partial charges in the resonance isomer lead to attraction between the two heteroatoms and thus a shorter O \cdots O distance, as indicated by the arrows in **2**.^{8c} In the second step, the positive hydrogen center moves toward the negatively charged hydrogen bond acceptor which leads to a quenching of the opposite charges and allows the π -delocalization to proceed further.^{8a,b} From an empirical model for partition of the hydrogen bonding energy, Gilli *et al.* proposed that the short strong hydrogen bond resulting from this feed-back mechanism gains its increased bond strength from the formation of an additional 3-center, 4-electron covalent contribution to the bonding picture.^{8c} A consequence of Gilli *et al.*'s proposal is that the atoms in the hydrogen-bonded moiety will have small or no partial charges at all,^{8c} and that the electrostatic stabiliza-

tion found in long weak hydrogen bonds is of no importance for the short strong bonds.



For benzoylacetone (**1** with $R_1 = \text{Ph}$ and $R_3 = \text{CH}_3$) the shape of the potential energy surface for the bridging hydrogen has been rationalized from a low-temperature (20 K) neutron diffraction study.⁹ On the basis of analysis of the thermal vibrations, it was possible to distinguish between the two viable scenarios of having either one almost symmetrical position or two disordered asymmetric positions for the hydrogen center in question.⁹ The study revealed that benzoylacetone has an ordered hydrogen positioned slightly closer to the phenyl-substituted C–O fragment than to the methyl group.⁹ By using this structure, the electron distribution was subsequently determined from a separate low-temperature (8 K) X-ray diffraction experiment.⁹ Madsen *et al.*⁹ were able to characterize the type of hydrogen bond found in benzoylacetone using Bader's¹⁰ Atoms in Molecules (AIM) theory. From an analysis of the electron density, strong evidence for covalent contributions to the bonds between the hydrogen center and both oxygens was found. The experimental data furthermore revealed that substantial partial charges are found on the oxygen and hydrogen atoms involved in the RAHB. On the basis of this observation, it was suggested that an RAHB yields a symmetrically charged molecule⁹ rather than a molecule where the charges are quenched, as suggested in the original formulation of RAHB.^{8a,b} These findings lead to a modification of the RAHB as displayed in **3**, with the partial charges included.⁹



The fundamental question of the shape of the potential energy surface for O \cdots H–O systems has been the topic of several theoretical studies concerning the simplest β -diketones, malonaldehyde¹¹ and acetylacetone,¹² as well as for other systems having negative charge-assisted short strong hydrogen bonds, e.g. the maleate ion,¹³ and the formate–formic acid¹⁴ and enol–enolate¹⁵ interactions. No definitive conclusions about the electronic structure of the short strong hydrogen bond present

(7) (a) Zhao, Q.; Abeygunawardana, C.; Talalay, P.; Mildvan, A. S. *Proc. Natl. Acad. Sci.* **1996**, *93*, 8220–8224. (b) Zhao, Q.; Abeygunawardana, C.; Gittis, A. G.; Mildvan, A. S. *Biochemistry* **1997**, *36*, 4616–4626. (c) Wu, Z. R.; Ebrahimian, S.; Zawrotny, M. E.; Thornburg, L. D.; Perez-Alvarado, G. C.; Brothers, P.; Pollack, R. M.; Summers, M. F. *Science* **1997**, *276*, 415–418.

(8) (a) Gilli, G.; Bellucci, F.; Ferretti, V.; Bertolasi, V. *J. Am. Chem. Soc.* **1989**, *111*, 1023–1028. (b) Bertolasi, V.; Gilli, P.; Ferretti, V.; Gilli, G. *J. Am. Chem. Soc.* **1991**, *113*, 4917–4925. (c) Gilli, P.; Bertolasi, V.; Ferretti, V.; Gilli, G. *J. Am. Chem. Soc.* **1994**, *116*, 909–915. (d) Gilli, G.; Bertolasi, V.; Ferretti, V.; Gilli, P. *Acta Crystallogr.* **1993**, *B49*, 564–576. (e) Bertolasi, V.; Gilli, P.; Ferretti, V.; Gilli, G. *Chem. Eur. J.* **1996**, *2*, 925–934. (f) Bertolasi, V.; Gilli, P.; Ferretti, V.; Gilli, G. *J. Chem. Soc., Perkin Trans. 2* **1997**, 945–952. (g) Bertolasi, V.; Nanni, L.; Gilli, P.; Ferretti, V.; Gilli, G.; Issa, Y. M.; Sherif, O. E. *New J. Chem.* **1994**, *18*, 251–261.

(9) (a) Madsen, G. K. H.; Iversen, B. B.; Larsen, F. K.; Kapon, M.; Reisner, G. M.; Herbststein, F. H. *J. Am. Chem. Soc.* **1998**, *120*, 10040–10045. (b) Madsen, G. K. H. Part A Thesis, University of Aarhus, Denmark, 1996.

(10) Bader, R. F. W. *Atoms in Molecules. A Quantum Theory*; Oxford University Press: New York, 1990.

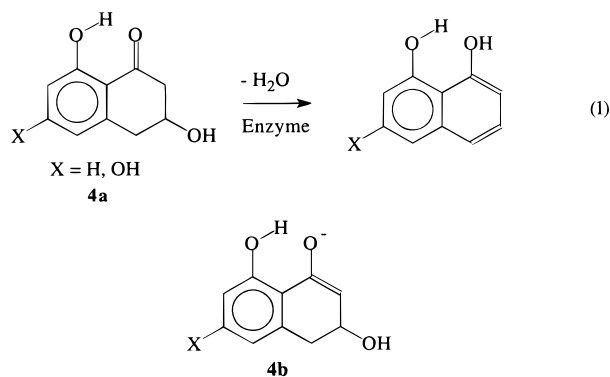
(11) (a) Frisch, M. J.; Scheiner, A. C.; Schaefer, H. F., III; Binkley, J. S. *J. Chem. Phys.* **1985**, *82*, 4194–4198. (b) Rios, M. A.; Rodriguez, J. J. *Mol. Struct. (THEOCHEM)* **1991**, *228*, 149–150. (c) Barone, V.; Adamo, C. *J. Chem. Phys.* **1996**, *105*, 11007–11019.

(12) Dannenberg, J. J.; Rios, R. J. *Phys. Chem.* **1994**, *98*, 6714–6718.

(13) (a) Garcia-Viloca, M.; Gonzalez-Lafont, A.; Lluch, J. M. *J. Am. Chem. Soc.* **1997**, *119*, 1081–1086. (b) McAllister, M. A. *Can. J. Chem.* **1997**, *75*, 1195–1202. (c) Alagano, G.; Ghio, C.; Kollmann, P. A. *J. Am. Chem. Soc.* **1995**, *117*, 9855–9862.

in these systems can be extracted from these studies. The general trend, though, is that electron correlation is essential for modeling adequately the hydrogen-bonded moiety to give structures that are comparable to experimental results.^{11–15}

At least one enzyme is known to involve the keto–enol form of a β -diketone in the active site, namely scytalone dehydratase,^{16a} which catalyzes the dehydration of two intermediates, **4a**, in the biosynthesis of melanin, reaction 1. A key step in the proposed reaction mechanism is the formation of the enolic intermediate, **4b**, by abstraction of the α -proton. Structures **4a**



and **4b** both contain a cis- β -keto–enol fragment, and similar structures were included by Gilli et al. in their correlation study of the O...O distance versus hydrogen bond strength.^{8f} Zheng and Bruce have studied the reaction mechanism by ab initio methods; they found that at the HF/6-31G(d) level of theory bond distances for the hydrogen-bonded O...H–O moiety are within the limits of potential formation of a short strong hydrogen bond.^{16b}

We have conducted a theoretical study of the structure of benzoylacetone, focusing on the type of hydrogen bond present. To the best of our knowledge, this is the first time high-level theoretical calculations on a molecular system with a short strong hydrogen bond are directly compared to accurate nuclear and electron distributions determined by very low-temperature neutron and X-ray diffraction. This enables us to check the theoretical method in use. Issues such as what model chemistry (methodology and basis set) has to be used to model the experimental structure will be discussed. Comparisons will be made to other theoretical studies of systems with short strong hydrogen bonds to formulate trends for the characteristic features of this type of bond. Finally, implications for enzymatic reactions for which low-barrier hydrogen bonds (LBHB) have been proposed will be discussed.

Computational Procedure

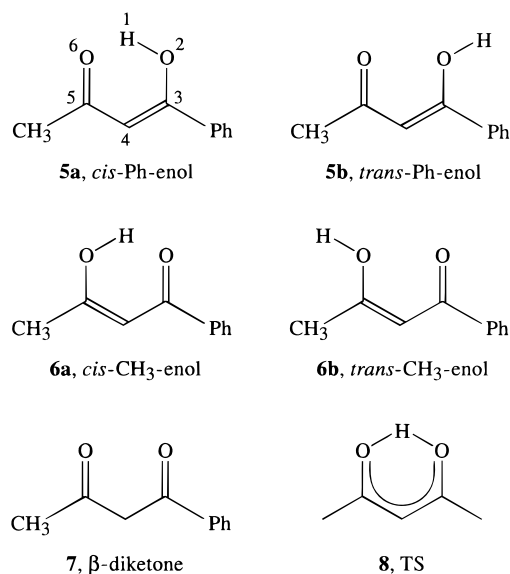
All ab initio calculations were performed with the Gaussian 94 suite of programs.¹⁷ The molecules studied are shown in Chart 1. All optimizations were conducted without constraints unless noted specifically. The two hydrogen-bonded cis- β -keto–enol isomers, **5a** and **6a**, were completely optimized at HF/6-31+G(d), B3LYP/6-31+G(d), and B3LYP/6-311G(d,p) levels of theory. Only when Density Functional Theory¹⁸ (DFT) with the rather large basis set, 6-311G(d,p), was used

(14) (a) Basch, H.; Stevens, W. J. *J. Am. Chem. Soc.* **1991**, *113*, 95–101. (b) Pan, Y.; McAllister, M. A. *J. Am. Chem. Soc.* **1997**, *119*, 7561–7566. (c) Pan, Y.; McAllister, M. A. *J. Am. Chem. Soc.* **1998**, *120*, 166–169. (d) Smallwood, C. J.; McAllister, M. A. *J. Am. Chem. Soc.* **1997**, *119*, 11277–11281. (e) Kumar, G. A.; McAllister, M. A. *J. Am. Chem. Soc.* **1998**, *120*, 3159–3165.

(15) Pan, Y.; McAllister, M. A. *J. Org. Chem.* **1997**, *62*, 8171–8176.

(16) (a) Lundquist, T.; Rice, J.; Hodge, C. N.; Basarab, G. S.; Pierce, J.; Lindquist, Y. *Structure* **1994**, *2*, 937. (b) Zheng, Y.-J.; Bruce, T. C. *Proc. Natl. Acad. Sci.* **1998**, *95*, 4158–4163.

Chart 1



did the optimized structures of **5a** and **6a** have an oxygen–oxygen separation similar to the experimental distance of 2.502(4) Å.⁹ This finding agrees well with the conclusions drawn from the extensive study on malonaldehyde (**1** with $R_1 = R_2 = R_3 = H$) at several very high levels of theory conducted by Adamo and Barone,^{11c} who found B3LYP/6-311G(d,p) to be the best compromise between accuracy of calculation and cost of computation. For intermolecular hydrogen-bonded systems, it has recently been shown that the B3LYP hybrid functionals^{19,20} represent a very good method for structural optimizations.²¹ To evaluate the strength of the intramolecular hydrogen bond the rotameric *trans*-isomers, **5b** and **6b**, and the β -diketone, **7**, were optimized at the B3LYP/6-311G(d,p) level of theory. The transition state, **8**, for the intramolecular hydrogen transfer from **5a** to **6a** was localized by using the Synchronous Transit-guided Quasi-Newton²² (STQN) technique at the B3LYP/6-311G(d,p) level of theory, as the traditional method using the Berny algorithm²³ failed. All stationary points were characterized by frequency analyses: true minima as having no imaginary frequencies and transition states as having exactly one imaginary frequency. For all saddle points, the imaginary frequency produced was analyzed by the XVibs program²⁴ to confirm that the located TS in fact corresponds to the internal hydrogen transfer and not, e.g., to a methyl rotation. For evaluation of the type of potential energy surface, the zero-point vibrational energies obtained in the frequency calculations were included. The frequencies which correspond to the O–H stretches of structures **5a** and **6a** were identified

(17) Gaussian 94, Revision B.2, Frisch, M. J.; Trucks, G. W.; Schlegel, H. B.; Gill, P. M. W.; Johnson, B. G.; Robb, M. A.; Cheeseman, J. R.; Keith, T.; Petersson, G. A.; Montgomery, J. A.; Raghavachari, K.; Al-Laham, M. A.; Zakrzewski, V. G.; Ortiz, J. V.; Foresman, J. B.; Cioslowski, J.; Stefanov, B. B.; Nanayakkara, A.; Challacombe, M.; Peng, C. Y.; Ayala, P. Y.; Chen, W.; Wong, M. W.; Andres, J. L.; Replogle, E. S.; Gomperts, R.; Martin, R. L.; Fox, D. J.; Binkley, J. S.; Defrees, D. J.; Baker, J.; Stewart, J. J. P.; Head-Gordon, M.; Gonzalez, C.; Pople, J. A.; Gaussian, Inc.: Pittsburgh, PA, 1995.

(18) (a) Kohn, W.; Sham, L. J. *Phys. Rev.* **1965**, *140*, A1133–A1138. (b) Parr, R. G.; Yang, W. *Density-functional theory of atoms and molecules*; Oxford University Press: Oxford, 1989.

(19) Becke, A. D. *J. Chem. Phys.* **1993**, *98*, 5648–5652.

(20) Lee, C.; Yang, W.; Parr, R. G. *Phys. Rev. B* **1988**, *37*, 785–789.

(21) (a) Lozynski, M.; Rusinska-Raszak, D.; Mack, H.-G. *J. Phys. Chem. A* **1998**, *102*, 2899–2903. (b) Novoa, J. J.; Sosa, C. *J. Phys. Chem.* **1995**, *99*, 15837–15845.

(22) Peng, C.; Ayala, P. Y.; Schlegel, H. B.; Frisch, M. J. *J. Comput. Chem.* **1996**, *17*, 49–56. Peng, C.; Schlegel, H. B. *Isr. J. Chem.* **1993**, *33*, 449–454.

(23) Foresman, J. B., Frisch, M. *Exploring Chemistry with Electronic Structure Methods*, 2nd ed.; Gaussian, Inc.: Pittsburgh, PA, 1995–96.

(24) XVibs 4.0.1, 1997, Hodoscek, M.; the program is available through the Computational Chemistry List maintained at the Ohio Supercomputer Center.

Table 1. The Intramolecular Oxygen–Oxygen Distance (Å) Calculated at Several Levels of Theory for the Two Isomers **5a** and **6a**

	Ph-enol, 5a	CH ₃ -enol, 6a
HF/6-31+G(d,p)	2.614	2.602
B3LYP/6-31+G(d,p)	2.534	2.541
B3LYP/6-311 G(d,p)	2.509	2.519
B3LYP/6-311 G(d,p) ^a	2.501	not converged

^a With the dihedral angle of the phenyl and methyl groups constrained to the experimental values.⁹

by XVibs²⁴ and visualized by XMol,²⁵ and their energies were computed and compared to the barrier height for hydrogen transfer.

As a goal of this study was to evaluate the type of bonds found in short strong hydrogen bonds, a topological analysis of the B3LYP/6-311G(d,p) electron density was performed with Bader's Atoms in Molecules (AIM) theory.¹⁰ According to this theory, all topological species (atoms, bonds, rings, etc.) that constitute a structure are uniquely defined from the electron density, ρ , of a molecular system. Structural elements are identified at critical points of the electron density distribution ($\nabla\rho = 0$), with atoms corresponding to local maxima, bonds and rings corresponding to saddle points, and cages corresponding to local minima. The sign of the Laplacian, $\nabla^2\rho$, of the electron density at a bond critical point reveals whether the charge is concentrated, as in covalent bonds ($\nabla^2\rho < 0$), or depleted, as in electrostatic bonds ($\nabla^2\rho > 0$). Thus, the AIM theory provides a tool for describing the nature of the bonds between the two oxygens and the hydrogen center in benzoylacetone. The AIM calculations were performed by using the critical point option for the AIM keyword as implemented in Gaussian 94.²⁶

Results and Discussion

Model Chemistry. One of the properties that so far seem to characterize short strong hydrogen bonds is the distance between the donor and acceptor.^{8,27} Geometry analyses at the minimum energy structures of the two *cis*- β -keto-enol isomers, **5a** and **6a**, were conducted at several levels of theory to determine the minimum level of theory necessary for theoretically reconstructing the accurate experimentally determined oxygen–oxygen separation of 2.502(4) Å.⁹ The optimized distances are shown in Table 1 for this crucial O...O contact at the various levels of theory.

The Hartree–Fock *ab initio* approaches overestimate the O...O separation by about 0.1 Å at the HF/6-31+G(d) level of theory. The inclusion of electron correlation through the B3LYP hybrid functionals greatly improved the optimized distance, by decreasing the O...O separation to 2.53–2.54 Å for the *cis*-keto-enol isomers. Changing to the triple- ζ basis set, 6-311G(d,p), gave values closer to the experimental distance of 2.502(4) Å⁹ with computed distances between the two oxygen centers for **5a** and **6a** of 2.509 and 2.519 Å, respectively. Due to the large size of the molecule, we decided to stay with this model, as optimizations with larger basis sets than the 6-311G(d,p) would be too expensive in computer time.^{11c}

(25) XMol 1.3.1, 1993, Wasikowski, C., Klemm, S.; Research Equipment, Inc. d/b/a Minnesota Supercomputer Center, Inc.

(26) (a) Cioslowski, J.; Nanayakkara, A.; Challacombe, M. *Chem Phys. Lett.* **1993**, *203*, 137–142. (b) Cioslowski, J.; Surjan, P. R. *J. Mol. Struct.* **1992**, *255*, 9. (c) Cioslowski, J.; Stefanov, B. B. *Mol. Phys.* **1995**, *84*, 707–716. (d) Stefanov, B. B.; Cioslowski, J. *J. Comput. Chem.* **1995**, *16*, 1394–1404. (e) Cioslowski, J. *Int. J. Quantum Chem. Quantum Chem. Symp.* **1990**, *24*, 15–28. (f) Cioslowski, J.; Mixon, S. T. *J. Am. Chem. Soc.* **1991**, *113*, 4142–4145. (g) Cioslowski, J. *Chem. Phys. Lett.* **1992**, *194*, 73–78; **1994**, *219*, 151–154.

(27) (a) Steiner, T.; Saenger, W. *Acta Crystallogr. Sect. B* **1994**, *50*, 348–357. (b) Kreevoy, M. M.; Marimanikkuppan, S.; Young, V. G.; Baranm J.; Szafran, M.; Schultz, A. J.; Trouw, F. *Ber. Bunsen-Phys. Chem., Chem. Phys.* **1998**, *102*, 370–376.

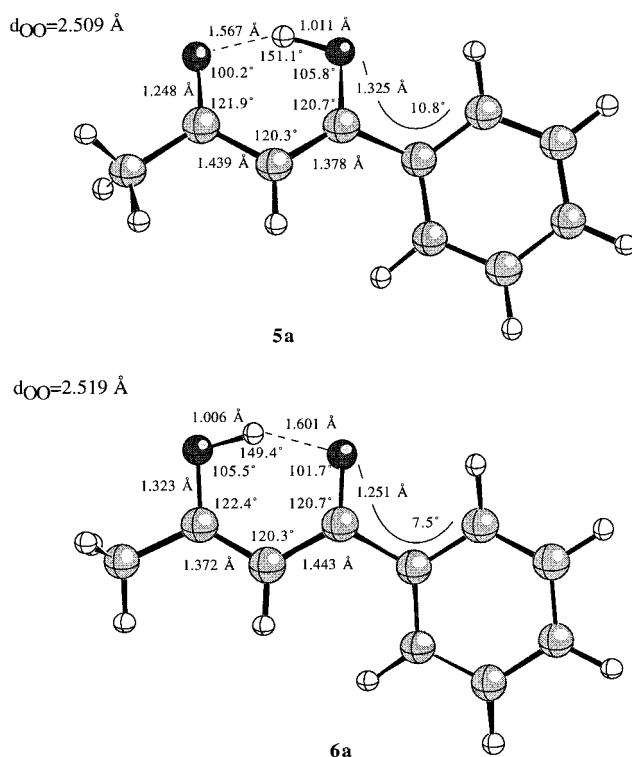


Figure 1. Optimized structures for **5a** and **6a** at the B3LYP/6-311G(d,p) level of theory.

Structural Analysis. The fully optimized structures of **5a** and **6a** are displayed in Figure 1 with essential bond distances, bond angles, and dihedral angles shown. The calculated O...O separations of the two *cis*-enol isomers of benzoylacetone are very similar to O...O distances calculated by McAllister et al. for negatively charge-assisted hydrogen-bonded systems such as the formic acid–formate system.^{14b} Upon binding of a water molecule this system gets a pK_a mismatch, and the O...O distance increases from around 2.4 Å for the pK_a -matched interaction of formic acid and formate to around 2.5 Å.^{14b–e} Benzoylacetone is a pK_a -mismatched system due to the different R¹ and R³ groups. Even though charge-assisted hydrogen-bonded systems generally have a shorter O...O separation,^{8c} this RAHB molecule is just as contracted as the (–)CAHB. When compared to pK_a -matched RAHB systems such as malonaldehyde^{11a,e} (R¹ = R³ = H) and acetylacetone¹² (R¹ = R³ = CH₃), it is striking to see that the theoretical O...O separations are longer (2.55–2.58 Å) in the pK_a -matched systems than in benzoylacetone at all levels of theory studied, including MP2 and DFT.^{11a,c} This observation may be rationalized through the fact that there is no steric compression in malonaldehyde, whereas the *ortho* hydrogens of the phenyl group in benzoylacetone can impose some strain onto the keto-enol moiety of the molecule. There have been discussions in the literature suggesting that relief of steric strain can be a driving force for the formation of short strong hydrogen bonds in proton sponges²⁸ and in the catalytic triad in the active site of serine proteases.^{6d}

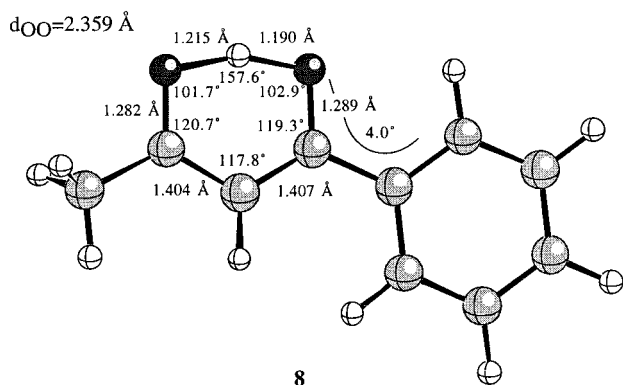
Both keto-enol isomers of Figure 1 have localized π -bonds in the *pseudo*-six-membered ring, held together by the intramolecular hydrogen bond. To prevent a too close contact between the α -hydrogen and the *ortho* hydrogen of the phenyl ring, structures **5a** and **6a** are not perfectly planar. In **5a**, the phenyl group is rotated by 10.8° relative to the keto-enol fragment of

(28) (a) Alder, R. W. *Chem. Rev.* **1989**, *89*, 1215–1223. (b) Perrin, C. L. *Annu. Rev. Phys. Chem.* **1997**, *48*, 511–544.

Table 2. Calculated Total Electronic Energies for **5a**, **5b**, **6a**, **6b**, **7**, and **8** at the B3LYP/6-311 G(d,p) Level of Theory (in hartrees, 1 hartree = 627.5 kcal/mol)^a

	<i>cis</i> -isomer, a	<i>trans</i> -isomer, b	E_{HB}
Ph-enol, 5	-537.683663	-537.657618	16.3
CH ₃ -enol, 6	-537.684843	-537.657850	16.2
β -diketon, 7	-537.674362		
TS, 8	-537.681021		

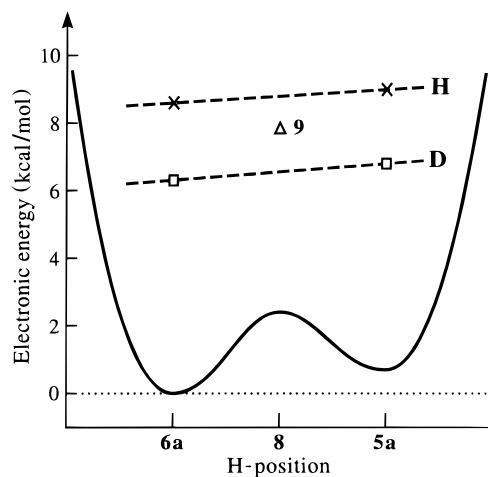
^a The hydrogen bond energies listed are found as the differences in energy between **5a** and **5b** for the Ph-enol isomer and between **6a** and **6b** for the CH₃-enol isomer. Absolute numbers are in hartrees, hydrogen bond energy in kcal/mol.

**Figure 2.** Optimized structure of the transition state, **8**, for transfer of the hydrogen from **5a** to **6a**.

the molecule, whereas this dihedral angle was computed to be 7.5° in **6a**. A slightly longer O—H bond length is found in the phenol-enol, **5a** (1.011 Å), compared to the methyl-enol isomer, **6a** (1.006 Å). On the other hand, the O...H distance shows the opposite behavior, **5a** has the shorter distance (1.567 Å) compared to the methyl-enol isomer, **6a** (1.601 Å). This may indicate a slightly more shared proton for the phenol-enol isomer. The computed numbers for bond distances of the O...H—O moiety of the two *cis*-enol isomers are in very good agreement with the experimental correlations established from a survey of several low-temperature neutron diffraction structures between O—H, O...H, and O...O distances.^{27a}

Table 2 lists the computed total potential energies for the structures of Chart 1. It is seen, that the *cis*-methyl-enol isomer is slightly favored over the *cis*-phenol-enol isomer by only 0.7 kcal/mol. The strength of the short strong resonance assisted hydrogen bond is estimated to be approximately 16 kcal/mol by comparing the total energies of **5a** and **6a** with those of **5b** and **6b**. This is considerably more than the energy of a normal hydrogen bond (2–10 kcal/mol).⁵ On the other hand, theoretical studies on negative charge assisted hydrogen bonds give bond strength of as much as 26–27 kcal/mol.^{12–14}

Potential Energy Surface. Following Hibbert and Emsley's^{5b} division of hydrogen bonds according to the shape of the PES, the energy of the O—H zero-point vibration, and the energy of the TS for hydrogen transfer, we next need to locate the TS of the intramolecular hydrogen transfer. The obtained structure of the TS is displayed in Figure 2. The TS has an O...O separation of 2.359 Å, which is very similar to computed values in other keto-enol systems.^{11,12} Two almost identical hydrogen-oxygen separations of 1.190 and 1.215 Å were calculated, showing that the hydrogen is slightly asymmetric, being a little closer to the phenyl side of the *pseudo*-six-membered ring, as predicted by Gilli et al.^{8a,b} The two C—C bond distances of the *pseudo*-six-membered ring are also almost identical, 1.407 and 1.405 Å, which is between a carbon-carbon single and

**Figure 3.** The calculated shape of the potential energy surface at the B3LYP/6-311G(d,p) level of theory. The crosses indicate the computed O—H vibrational energies whereas the squares indicate the O—D vibrational energies. The energy of the experimental structure is marked by a triangle.

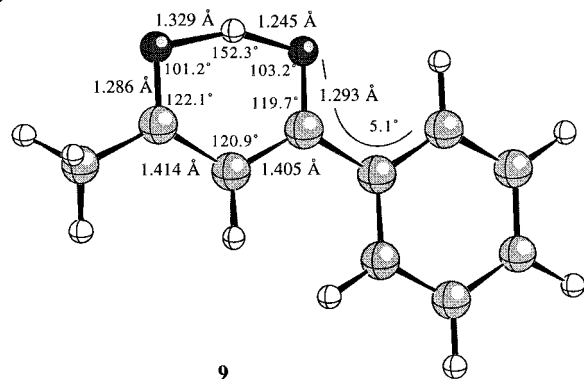
double bond. Similarly, the two carbon-oxygen distances are also almost identical with values between normal carbon-oxygen single and double bonds. The computed distances of the six-membered ring in the TS suggest that in this structure π -delocalization is found, in agreement with the RAHB model.^{8a-c} The angle around the transferring hydrogen is 157.6°. When compared to the two enol isomers, **5a** and **6a** of Figure 1, it is seen that the dihedral angle between the phenyl ring and the keto-enol moiety in the TS is decreased from 10.8° and 7.5° in **5a** and **6a**, respectively, to 4.0°. This may indicate that upon formation of the short strong hydrogen bond, steric repulsion between the phenyl group and the keto-enol fragment is released, thereby allowing the molecule to become more planar. The barrier for transfer of the hydrogen is computed to be 1.7 kcal/mol from **5a** to **6a** and 2.4 kcal/mol in the opposite direction. The emerging classical potential energy surface is sketched in Figure 3.

From an analysis of the vibrational energies computed in the harmonic approximation, the O—H stretching frequency was identified in **5a** and **6a**. The computed frequencies are $\nu_{\text{OH}}(\mathbf{5a}) = 2915.4 \text{ cm}^{-1}$ and $\nu_{\text{OH}}(\mathbf{6a}) = 3005.6 \text{ cm}^{-1}$; no scaling factor was used. For an isotopically substituted system, the O—D frequencies are $\nu_{\text{OD}}(\mathbf{5a}) = 2139.3 \text{ cm}^{-1}$ and $\nu_{\text{OD}}(\mathbf{6a}) = 2199.6 \text{ cm}^{-1}$. These approximate zero-point energies are marked in Figure 3 by crosses for the H-isotope and by squares for the D-isotope. As can be seen, both the O—H and the O—D zero-point vibration energies are located above the TS energy giving rise to what Hibbert and Emsley term as a very strong hydrogen bond.^{5b} This finding indicates that in benzoylacetone at 0 K, only one position is found for the hydrogen, in excellent agreement with the experimental low-temperature structure (20 K).⁹ An approximate shape of the emerging PES can be suggested by adding the computed zero-point vibration energies to the electronic energies.²⁹ The values are shown in Table 3. By doing so, the delocalized π -conjugated TS structure, **8**, has a slightly lower energy than the two *cis*- β -keto-enol isomers,

(29) The values of the ZPVE should be taken with caution since they are based on a harmonic model. It is likely that the PES contains considerable anharmonic components. However, the important point is the indication of a single well potential, which is in excellent agreement with the results of the neutron diffraction study. The same theoretical procedure has previously been applied by Garcia-Viloca *et al.*^{13a} in a study of the maleate ion. For a detailed discussion about the limitations of the harmonic model readers are referred to ref 13a.

Table 3. Calculated Potential Energy Barriers (kcal/mol) for the Intramolecular Hydrogen Transfer between **5a** and **6a**, without and with Zero-Point Vibrational Energies (ZPVE) Included

	no ZPVE	ZPVE included
5a → TS, 7	1.7	-0.6
6a → TS, 7	2.4	-0.2

 $d_{\text{OO}}=2.502 \text{ \AA}$ **Figure 4.** The experimental 20 K neutron structure of benzoylacetone⁹ with important bond distances and bond angles indicated.

5a and **6a**, leading to the conclusion that for benzoylacetone the intramolecular hydrogen bond is described as a single-well potential and the hydrogen is not shifting between two minima. In the following we will indicate this special type of hydrogen bond by $\text{O} \cdots \text{H}$ and $\text{O} \cdots \text{H} \cdots \text{O}$, a schematic representation that has been used widely for enzymatic reactions where the formation of LBHBs has been proposed.^{6d}

Experimentally, strong evidence for a single-well potential was found from a thermal vibration analysis of neutron diffraction data,⁹ which is in good agreement with the above analysis. The experimental structure, **9**, is shown in Figure 4. From the low-temperature (20 K) neutron diffraction experiment evidence for a slightly asymmetric hydrogen position was found. Upon comparison of **9** to the theoretical TS, **8**, some minor deviations are found in the $\text{O} \cdots \text{H} \cdots \text{O}$ region, while all other parts of the molecule have almost identical structural features. The experimental oxygen–oxygen separation is 2.502(4) Å compared to 2.359 Å in the TS. Other minor differences are found in the dihedral angles of the phenyl and methyl groups. These differences can most likely be explained by crystal packing effects. To check this hypothesis, a test run was done where a TS was localized having the Ph and CH₃ dihedrals constrained at the experimental values. The $\text{O} \cdots \text{O}$ separation found for the *cis*-phenyl-enol isomer is very similar to the experimental one, as a distance of 2.501 Å was computed, which has to be compared to 2.502(4) Å for the experimental structure.⁹ The *cis*-methyl-enol isomer could not be optimized due to problems with convergence, confirming the theoretical prediction of a very flat PES. Structurally, the constrained TS had no differences in the $\text{O} \cdots \text{H} \cdots \text{O}$ region compared to the unconstrained one, **8**. A single point calculation using the neutron structure was performed and the computed energy is marked by a triangle in Figure 3. The energy of the neutron structure falls almost on top of the dashed lines which indicates the O–H zero-point vibration energy, giving fine agreement between the B3LYP/6-311G(d,p) level of theory and the accurate low-temperature diffraction experiments.

Molecular Properties. While the nuclear positions compare well between theory and experiment, an additional check of the theoretical model was done by computing the molecular dipole moment, atomic charges, and properties of the electron density

Table 4. Calculated Dipole Moments (D) at the B3LYP/6-311G(d,p) Level of Theory^a

	Brenneman <i>et al.</i> ^{30b}	Merz–Kollman ^{30a}	Mulliken
5a	8.495	8.386	8.330
6a	7.704	7.635	7.596
8	8.261	8.167	8.126
9	8.258	8.165	8.108

^a The experimental value is 7(1) D.^{9b}**Table 5.** Calculated Atomic Charges at the B3LYP/6-311G(d,p) Level of Theory with Brenneman *et al.*'s Scheme for Fitting Atomic Charges from the Electrostatic Potential^a

atom	H ¹	O ²	O ⁶
5a	0.477	-0.571	-0.611
6a	0.453	-0.573	-0.573
5b	0.327	-0.403	-0.527
6b	0.406	-0.483	-0.522
8	0.490	-0.589	-0.608
9	0.451	-0.559	-0.593
expt ⁹	0.40(3)	-0.51(5)	-0.45(4)

^a Experimental charges are included for comparison. The atom numbering scheme corresponds to **5a**.

at the bond critical points of the structure. Table 4 lists the dipole moments for **5a**, **6a**, and **8** as well as a computed dipole moment for the experimental structure, **9**, at the B3LYP/6-311G(d,p) level of theory. Three different methods were included: Mulliken population analysis and two schemes for electrostatic potential fitting.³⁰ All methods and structures give a dipole moment close to the experimental value of 7(1) D, which was evaluated from the X-ray charge density distribution at 8 K.^{9b} It has been shown that dipole moments derived from multipole modeling of X-ray diffraction data are underestimated by 10–15%,³¹ which agrees well with the present findings. In Table 5, atomic charges are listed for the three atoms involved in the short strong hydrogen bond for the *cis*- and *trans*-keto–enols as well as for the TS and the experimental structure. The charges were calculated at the B3LYP/6-311G(d,p) level of theory by using Brenneman *et al.*'s scheme for fitting atomic charges to the electrostatic potential of a molecule.^{30b} Large atomic partial charges were found on the oxygens and the hydrogen atoms of the keto–enol group, in good agreement with the experimental finding.⁹ This suggests that a substantial electrostatic interaction is present in short strong hydrogen bonds. This is in contradiction with the RAHB model proposed by Gilli *et al.*,^{8c} and this finding formed the key basis for the revised RAHB model proposed by Madsen *et al.*,⁹ see **3**. To confirm further that large atomic charges are found in the RAHB, theoretical charges for **5b** and **6b** were computed to provide an internal reference for the applied method of computing charges. Indeed, when no intramolecular hydrogen bond is present, lower partial charges are found.

To determine the type of bonding present in the $\text{O} \cdots \text{H} \cdots \text{O}$ region, an Atoms in Molecules¹⁰ (AIM) investigation of the electron density at bond critical points was undertaken. The computed numbers for the electron density (ρ), the Laplacian ($\nabla^2\rho$), and the ellipticity (ϵ) are given in Table 6 for the computed TS structure, **8**, and for the experimental structure, **9**. The experimental values⁹ are also listed for comparison. In general, very good quantitative agreement between the high level ab initio electron density and the X-ray electron density is found.

(30) (a) Besler, B. H.; Merz, K. M.; Kollmann, P. A. *J. Comput. Chem.* **1990**, *11*, 431–439. (b) Breneman, C. M.; Wiberg, K. B. *J. Comput. Chem.* **1990**, *11*, 361–373.(31) Spackman, M. A.; Byrom, P. G. *Acta Crystallogr. Sect. B* **1996**, *52*, 1023–1035.

Table 6. Properties of the Electron Density at Bond Critical Points for the Transition State Structure, **8**, and the Experimental Structure, **9**, at the B3LYP/6-311G(d,p) Level of Theory^a

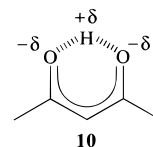
		$\rho/e\text{\AA}^{-3}$	$\nabla^2\rho/e\text{\AA}^{-5}$	ϵ
H ¹ ...O ²	8	1.240	-8.45	0.013
	9	1.084	-6.34	0.010
	9 ⁹	0.89(3)	-9.1(2)	0.15
O ² -C ³	8	2.324	-9.11	0.012
	9	2.312	-9.02	0.014
	9 ⁹	2.44(8)	-26.0(4)	0.21
C ³ -C ⁴	8	2.050	-20.04	0.242
	9	2.057	-20.14	0.250
	9 ⁹	2.17(4)	-18.20(9)	0.29
C ⁴ -C ⁵	8	2.062	-20.16	0.254
	9	2.026	-19.49	0.246
	9 ⁹	2.04(4)	-16.15(9)	0.25
C ⁵ -O ⁶	8	2.360	-8.53	0.008
	9	2.354	-9.14	0.004
	9 ⁹	2.54(8)	-29.0(4)	0.10
O ⁶ -H ¹	8	1.160	-5.65	0.011
	9	0.871	-10.91	0.013
	9 ⁹	0.76(3)	-4.5(2)	0.10

^a The first entry under each bond refers to **8**, the second to the computed value for **9**, and the third to the experimental value.⁹ The atom numbering scheme corresponds to **5a**.

The negative values of the Laplacian at the critical point of both O^{||||}H bonds of **8** and **9** show that the hydrogen is stabilized by covalent bonding contributions to both oxygens. There is a difference between the experimental and theoretical values of ρ at the bond critical points of **9**, with the theoretical values being a little higher. The computations, therefore, suggest that slightly more covalent character is associated with the O^{||||}H bonds when compared with the experiment; this is also to be expected from the shorter O-H bond distances calculated for **8** compared with the experimental structure, **9**. The lower absolute values of the theoretical Laplacians of the C-O bonds of **8** and **9** may not be correct, since a strong covalent bond is expected between carbon and oxygen based on the computed bond distances for **8**.

For the C-C bonds, the AIM ellipticities show a perfect match between theory and experiment,⁹ revealing the π -delocalization over both C-C bonds. However, the theoretical ellipticities for the C-O bond at the B3LYP/6-311G(d,p) level of theory are very small. The RAHB model predicts delocalization over all heteroatoms in the keto-enol fragment and we expect to see some ellipticity in the C-O bonds, as is indeed the case for the X-ray charge density.⁹ To test whether the low C-O ellipticity is due to an inadequate modeling of the hydrogen-bonded region, a single point calculation at the B3LYP/6-311++G(2d,p) level of theory was carried out with use of the experimental geometry, **9**. At this level of theory the ellipticities of the C-O bonds have only increased to 0.03 and 0.04. However, it should be noted that Cheeseman et al. have shown that in the case of heteroatomic bonds having large charge transfer, the ellipticity at the bond critical point is not a sensitive indicator of π -contributions to the bonding.³² Rather they suggest to look at the ellipticity over the entire bond.³² Second, because the ellipticity is the ratio between two second derivatives of the electron density, it is a feature that is very difficult to determine accurately. The X-ray experiment shows some ellipticity in the O^{||||}H bonds that is not reproduced by theory. The experimental values are relatively inaccurate since the critical points of the O^{||||}H bonds are found in the low-density region of the structure.⁹ On the basis of the present

theoretical and experimental evidence it seems that there is only weak, if any, π -delocalization over the O-H bonds. The ellipticity of the true σ -type O-H bond in **5a** and **6a** is identical to the numbers calculated for O^{||||}H in **8** and **9**, thus it seems that the symmetry character of the bond between oxygen and hydrogen is unchanged upon formation of the strong short hydrogen bond. This leads us to the conclusion that the O^{||||}H^{||||}O system in benzoylacetone is best described as a 3-center, 4-electron σ -bond with considerable polar character as drawn in **10**. The four electrons involved in the three-center bond may formally be attributed to the $\sigma_{\text{O-H}}$ orbital and one of the lone pairs at the carbonyl-oxygen center in one of the localized *cis*-keto-enol isomers, **5a** and **6a**.



Implications for LBHBs in Enzymatic Reactions. Garcia-Viloca et al.^{13a} studied the structure of the maleate ion. They found that the barrier to intramolecular hydrogen transfer is small and vanishes when zero-point vibrational energies are considered.^{13a} This is very similar to what was found here for benzoylacetone. A topological analysis of the electron density of the TS for the intramolecular hydrogen transfer in the maleate ion^{13a} gave values for ρ of 1.215 and $-10.6 e/\text{\AA}^5$ for $\nabla^2\rho$ at the two O-H bond critical points, both of which were positioned close to the hydrogen center.^{13a} These results are very similar to the findings reported in this study. Since the electron densities in the short strong hydrogen bonds are similar for both the maleate ion and benzoylacetone, one can speculate that the bonding found in the two systems is similar. This suggests that the electronic nature of a short strong hydrogen bond may be independent of how charges are formally assigned for the system—a conclusion that was also reached by Gilli et al. based on a completely different type of analysis.^{8c} As a consequence of this, the findings in the present study may be extrapolated to enzymatic systems where LBHBs have been suggested. This means that an LBHB in an enzymatic active site can be expected to have covalent bonding contributions between the hydrogen and both heteroatoms involved, which was originally suggested by Cleland and Kreevoy^{6c} and by Frey et al.^{6e} Our studies of benzoylacetone furthermore show that the atoms involved in LBHBs may also carry substantial charges, an observation that has not previously been realized. The present study reveals that the electrostatic contribution to the hydrogen bond may play a significant role in LBHBs because the involved atoms have large partial charges, but the analysis of the charge distributions clearly shows that the fundamental electronic character of the two hydrogen bonds has changed to include a covalent component as well. Therefore, one should include the possibility of studying nonelectrostatic changes, such as charge transfer and structural changes, when modeling systems with short strong hydrogen bonds or LBHBs. The formation of two partly covalent bonds to the bridging hydrogen center results in a very deshielded proton and large partial charges on the hydrogen bonded atoms. This is in agreement with the experimental very high ¹H chemical shifts measured by NMR for LBHB protons.

Conclusions

The present study demonstrates that the short intramolecular hydrogen bond in benzoylacetone is a low barrier hydrogen

(32) Cheeseman, J. R.; Carroll, M. T.; Bader, R. F. W. *Chem. Phys. Lett.* **1988**, *143*, 450-458.

bond, as a double-well potential is found with a low barrier to internal hydrogen transfer. Detailed comparison with nuclear and electron densities determined from very low-temperature diffraction experiments shows that theoretical studies of short hydrogen bonds need to include electron correlation effects and employ large basis sets. Good quantitative agreement is found between the B3LYP/6-311G(d,p) level of theory and the X-ray charge density for most of the compared properties. Some discrepancy is found for certain very demanding electronic properties such as the ellipticity of the C–O bonds. It is therefore desirable to carry out other detailed comparisons between high level theoretical calculations and accurate diffraction studies to further validate the *ab initio* density functional theoretical approach.

The study has found that the RAHB system in benzoylacetone possesses large atomic partial charges on the O····H····O fragment. Furthermore, an AIM analysis of the electron density at the bond critical points revealed that covalency is important for describing the interaction between hydrogen and both oxygen centers, as originally proposed by Gilli and co-workers.⁸ The hydrogen is stabilized by bonds to both oxygen atoms which contain covalent as well as electrostatic contributions. The π -delocalization is found over the carbon and oxygen atoms in the keto–enol ring but not over the O····H bonds, as judged from a combined analysis of the calculated bond distances and ellipticities. The O····H····O bond is therefore best described as a 3-center, 4-electron σ -bond with considerable polar character.

When comparing the results in this study to structural information of other keto–enol systems it becomes apparent that the pK_a match/mismatch may not be the only determining factor⁶ for establishing a short strong hydrogen bond or an LBHB, as the pK_a -matched molecules malonaldehyde and acetaldehyde have longer O····O separations than the pK_a -mismatched benzoylacetone. Relief of steric strain in benzoylacetone upon formation of the short hydrogen bond can be used to explain this unexpected finding, and supports Frey *et al.*'s refined mechanism for the formation of an LBHB between the catalytic triad histidine and aspartate in serine proteases.^{6f} The study also indicates that LBHBs in enzymes, at least the heteroatomic O–H····O[–] systems, such as Δ^5 -3-ketosteroid isomerase,⁷ scytalone dehydratase,²² and others,^{6c} may indeed have large partial charges on the three hydrogen bonded atoms, and not largely uncharged as previously believed.⁶ Further investigations focusing on the electronic nature and energetics of short strong hydrogen bonds and LBHBs are in progress in our laboratories.

Acknowledgment. This work was supported by grants from the NIH (DK09171) and from the National Center for Supercomputing Applications, Urbana–Champaign, IL (CHE980023N). B.S. and B.B.I. thank the Danish Natural Science Research Council and the Carlsberg Foundation for providing postdoctoral fellowships.

JA982317T